Land subsidence in Mashhad Valley, northeast Iran: results from InSAR, levelling and GPS

Mahdi Motagh,[1] Yahya Djamour,[2] Thomas R. Walter,[1] Hans-Ulrich Wetzel,[1] Jochen Zschau[1] and Siavash Arabi[2]

[1]*GeoForschungsZentrum, D-14473 Potsdam, Germany. E-mail: motagh@gfz-potsdam.de*
[2]*National Cartographic Center of Iran, Tehran, Iran*

SUMMARY

Significant land subsidence was recently recognized in northeast Iran, near the city of Mashhad. Precise levelling surveys performed in 1995, 2002 and 2005, indicate as much as 90 cm of subsidence during the 1995–2005 period. Continuous GPS monitoring approximately 8 km northwest of Mashhad City shows more than 20 cm yr^{-1} subsidence between 2005 and 2006. We use Interferometric Synthetic Aperture Radar (InSAR) measurements to detect the temporal and spatial pattern of this surface deformation. 13 interferograms from 10 C-band SAR images acquired by the Enivsat satellite from 2003 to 2005 are analysed and stacked. Our InSAR mapping suggests that subsidence occurs within a northwest–southeast elongated elliptic-shaped bowl along the axis of the Mashhad valley, with a peak amplitude of $\sim$28–30 cm yr^{-1} for the 2003–2005 time period. The InSAR data indicate that approximately 70 km^2 in the valley floor, including the northwestern part of Mashhad City, subsided at a rate exceeding 15 cm yr^{-1} between 2003 and 2005, and that the subsidence area is structurally controlled by the trends of Quaternary faults cutting the valley floor. Analysis of piezometric records suggests that subsidence likely results from extensive overdrafting of the aquifer system in the valley that has caused as much as 65 m of water table decline since 1960s.

**Key words:** groundwater, InSAR, subsidence.

1 INTRODUCTION

Land-surface subsidence due to overextraction of groundwater has been long recognized as a potential problem in many areas that have undergone extensive groundwater development (e.g. Longfield 1932; Tolman & Poland 1940; Poland 1956; Poland & Davis 1969; Bull & Poland 1975; Ikehara & Philips 1994; Galloway *et al.* 1998, 1999; Abidin *et al.* 2001). In 1991, the US National Research Council placed the annual costs from flooding and structural damage caused by land subsidence within the United States alone at over $125 million. Geodetic measurement of surface deformation with sufficiently dense spatial and temporal coverage is essential for accurately assessing the magnitude, distribution and spatial pattern of land subsidence at groundwater basins. When combined with independent hydrologic and geologic measurements, such surface deformation may provide important insight about constitutive parameters controlling the extent, morphology and dynamics of underground aquifers (Poland 1984).

Interferometric Synthetic Aperture Radar (InSAR) provides a unique tool for detecting and monitoring deformation over regions of ongoing groundwater development. With its wide spatial coverage ($\sim$10^4 km^2), fine spatial resolution ($\sim$10^2 m^2), and high accuracy ($\sim$1 cm), InSAR offers new capabilities to measure surface deformation caused by aquifer discharge and recharge at an unprecedented level of detail never before possible with techniques like GPS and levelling (Galloway *et al.* 1998; Amelung *et al.* 1999; Hoffmann *et al.* 2001; Bell *et al.* 2002; Schmidt & Bürgmann 2003; Lanari *et al.* 2004). This paper is a case study showing how spatially dense InSAR results complement sparse geodetic measurements from GPS and levelling, and contribute to a better understanding of land subsidence associated with water extraction in the Mashhad area, northeast Iran.

The Valley of Mashhad is a northwest–southeast (NW–SE) trending valley in northeast Iran. It is a broad sedimentary basin composed primarily of Quaternary-Neogene alluvial deposits, bounded on the south by the Binalud Mountains and on the north by the Hezar-Masjed Mountains (Fig. 1a). The region is tectonically characterized by major active thrust zones of the Binalud and Kashafrud faults, running along the southern margin of the Binalud and Hezar-Masjed mountains, respectively, and a series of normal faults as well as basin boundary faults as shown in Fig. 1(a). The basin encompasses the city of Mashhad, a provincial capital inhabited by over 2 million people and visited annually by millions of tourists. Mashhad extends over an area of more than 200 km^2 across the basin, is the second largest city in Iran, and is one of the fastest-growing metropolitan areas in the nation. Groundwater has been an

(a)

(b)
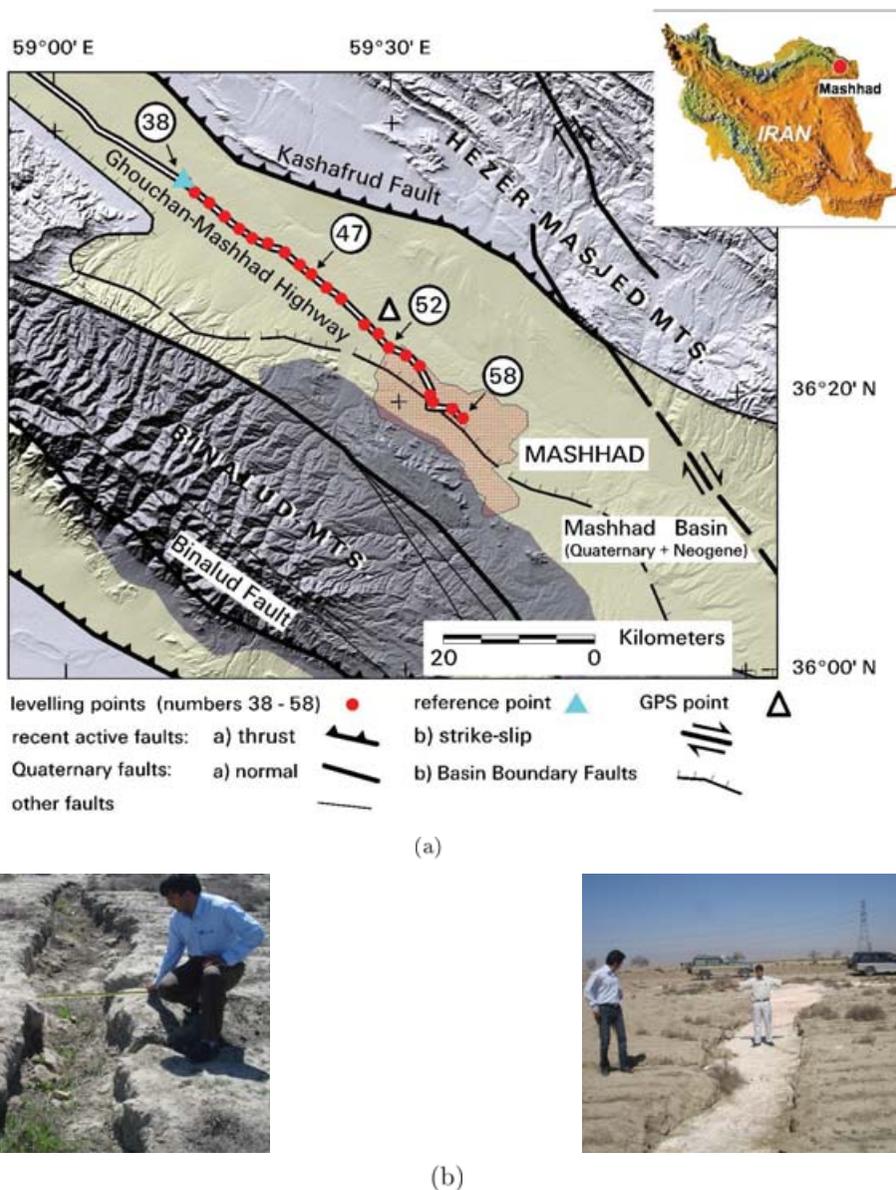
Figure 1. (a) Generalized geologic map of the Mashhad region based on the published 1:2,500,000-scale geological map from National Iranian Oil Company (NIOC), and the map of major active faults in Iran from International Institute of Earthquake Engineering and Seismology (IIEES). The map is overlain on a shaded-relief topographic image generated from the 3-arcsecond Shuttle Radar Topography Mission (SRTM) data. The inset shows the location of Fig. 1(a) within Iran. (b) Two examples of surface fissures in Mashhad Valley caused probably by excessive groundwater withdrawal and associated aquifer-system compaction. The fissures are located northwest of Mashhad City and to the east of the Tous GPS station marked by a triangle in Fig. 1(a).

important resource in the Mashhad region for domestic, industrial and agricultural water supplies. However, substantial exploitation of groundwater due to population growth, tourism and development, coupled with deficient natural recharge in recent decades, has resulted in severe depletion of the underground aquifer, leading to regional decline of water-table levels, lack of access to fresh water, and development of earth fissures and local sinking in many areas of the valley (Fig. 1b).

In this article, we first present evidence for the evolution of land subsidence in the Mashhad valley recorded from precise levelling and continuous GPS observations. As we shall see in Section 2, both levelling and GPS data indicate that substantial subsidence has been occurring in the region over the past years. Through interferometric observations in Section 3 we can quantify the magnitude and spatial extent of subsidence at Mashhad in much greater detail.

2 SUBSIDENCE IN MASHHAD FROM LEVELLING AND GPS

Geodetic observations of local land subsidence were first documented for the Mashhad region from precise levelling data collected by the National Cartographic Center of Iran (NCC) during 1995–2002 and 2002–2005 campaigns. Fig. 1(a) shows the location of levelling benchmarks extracted from ~50-km-long levelling line along the Ghouchan-Mashhad Highway. A number of stations were destroyed between 1995 and 2002 and NCC had to install a set of new benchmarks—namely BM46–BM49, BM54, BM55 and BM57- for the 2002–2005 campaign. The levelling surveys have been made to specifications required for first-order precise levelling; The expected standard error for the change in elevation difference between two benchmarks as measured in two surveys can be expressed as

(a)

(b)
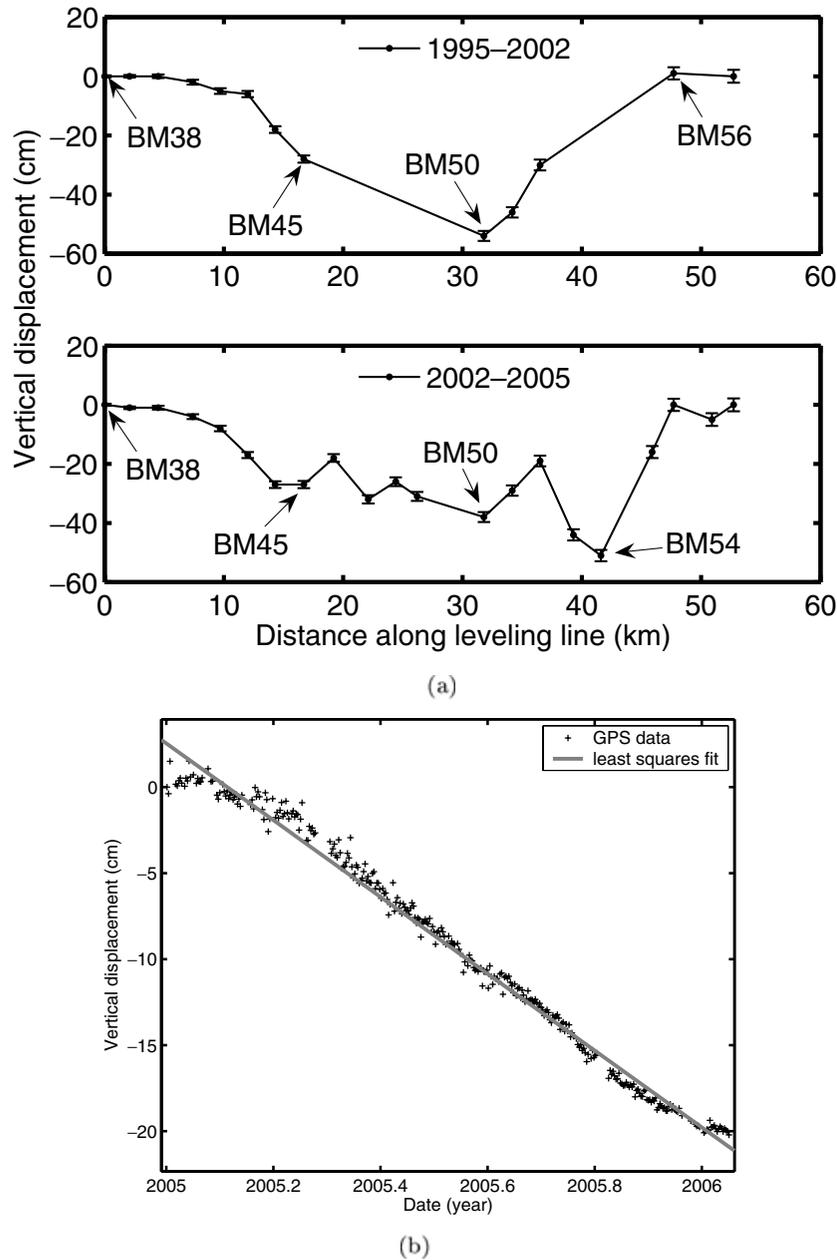
Figure 2. (a) Results of first-order precise levelling surveys in Mashhad Valley between 1995 and 2005 (see Fig. 1a for location of benchmarks). Error bars represent three standard deviations in cumulative random error from the reference benchmark ($\sigma = \pm \alpha L^{1/2}$, where $\alpha = 1$ mm/km$^{1/2}$ and L is the distance in kilometres along the levelling line between benchmarks). New benchmarks BM46-BM49, BM54, BM55 and BM57 only surveyed during the 2002–2005 campaign. (b) plot of GPS up component (in cm) for the Tous GPS station (triangle in Fig. 1a) with least-squares linear trend (slope ~22 cm yr^{-1}) overlain.

$\pm \alpha L^{1/2}$, where $\alpha = 1$ mm/km$^{1/2}$ and L is the distance in kilometres along the levelling line between benchmarks (Memarzadeh 1998).

The development of vertical deformation along the Ghouchan-Mashhad Highway between the 1995, 2002 and 2005 surveys relative to a datum at BM38 is shown in Fig. 2(a). Both surveys show a consistent pattern of subsidence for common benchmarks. For the 7-yr period 1995–2002, the maximum cumulative amount of subsidence recorded by a benchmark is as high as 58 cm at a point located approximately 6 km northwest of Mashhad City (BM50). For the 3-yr period 2002–2005, the survey exhibits a more complex pattern of subsidence along the levelling line than does the earlier 1995–2002 survey. A maximum of 51 cm of subsidence occurs in this period

at station BM54, located in the northwestern part of Mashhad City. The total subsidence of benchmark BM50 from 1995 to 2005 is 96 cm. The vertical displacements do not show correlation with topography, confirming that elevation-dependent systematic error is not involved in the levelling data.

In 2004, as part of a program to extend and densify the Iranian Permanent GPS Network for Geodynamic (IPGN), the NCC installed a continuously recording GPS station near the city of Tous, less than 10 km away from the levelling station BM50. The location of the GPS station is shown by a white triangle in Fig. 1(a). GPS measurements are made using a dual-frequency Ashtech Z-12 receiver and a choke-ring antenna at a 30 s sampling rate and

Table 1. Characteristics of interferograms used in this study.

Master orbit	Master date	Slave orbit	Slave date	Elapsed time (day)	B_{perp} (m)
6959	2003.06.30	9464	2003.12.22	175	~182
6959	2003.06.30	17 981	2005.08.08	770 (Fig. 3f)	~−116
8462	2003.10.13	11 969	2004.06.14	245	~−376
8462	2003.10.13	16 478	2005.04.25	560 (Fig. 3e)	~61
9464	2003.12.22	16 979	2005.05.30	525	~ −94
11 969	2004.06.14	13 973	2004.11.01	140 (Fig. 3c)	~130
11 969	2004.06.14	18 482	2005.09.12	455	~−52
11 969	2004.06.14	19 484	2005.11.21	525	~125
13 973	2004.11.01	16 478	2005.04.25	175	~261
13 973	2004.11.01	19 484	2005.11.21	385 (Fig. 3d)	~−28
16 979	2005.05.30	17 981	2005.08.08	70	~−194
16 979	2005.05.30	18 482	2005.09.12	105 (Fig. 3b)	~276
18 482	2005.09.12	19 484	2005.11.21	70 (Fig. 3a)	~165

processed at NCC using the GAMIT/GLOBK software (King & Bock 1995; Herring 1998). The GPS processing follows standard procedures as described in Feigl *et al.* (1993) and McClusky *et al.* (2000). First, by applying loose a priori constraints to all parameters, doubly differenced phase observations from each day are used to estimate daily coordinates, one tropospheric parameter every 2 h, and orbital and Earth orientation parameters (EOPs). A total of 20 reliable IGS stations are included within the analysis to strengthen the regional reference frame and constrain the orbital parameters. The loosely constrained estimates for station coordinates and corresponding matrices of the covariance among the three position components are then used as quasi-observations in a Kalman filter to estimate a consistent set of daily solutions for station positions within the ITRF2000 reference frame (Altamimi *et al.* 2002), which are then transformed into local coordinates to derive horizontal and vertical position variations. The results of continuous GPS observations at Tous station between 2005 and 2006, the longest time interval for which GPS data already acquired and processed at NCC at the time of this writing, indicates significant subsidence of approximately 22 cm at the station (Fig. 2b).

In the following, we investigate the subsidence in the Mashhad valley using surface displacement maps generated by InSAR. The advantages and complementary character of InSAR, which can provide a quasi-continuous and spatially dense map of displacement field over broad areas (e.g. Massonet *et al.* 1993; Peltzer *et al.* 1998; Bürgmann *et al.* 2002; Simons *et al.* 2002; Fialko 2006; Motagh *et al.* 2006), allow us to detect and analyse subsidence in the valley in far greater detail than currently possible with sparse ground—and satellite-based geodetic measurements from levelling and GPS.

3 INSAR OBSERVATIONS

To measure ground subsidence in the Mashhad valley we selected 10 Envisat SAR images (see Table 1) in descending orbits and used the so-called two-pass technique (Zebker *et al.* 1994) to generate a set of differential interferograms covering a time period between 2003 June 30 and 2005 November 21. Interferometric processing is done using the public domain InSAR processor DORIS developed at Delft Institute for Earth-oriented Space Research (Kampes & Usai 1999). The interferograms are corrected for the phase signature due to orbital separation using precise DEOS satellite orbits (Scharroo & Visser 1998), and for the topography using a 3-arcsecond SRTM digital elevation model (http://srtm.usgs.gov). We improve signal-to-noise ratio of each differential interferogram using a weighted power spectrum filter as discussed in Goldstein & Werner (1998).

Fig. 3 shows six geocoded differential interferograms of the 45 ones constructed using the two-pass method in this study. One complete cycle of colour corresponds to half a wavelength of apparent range change (~28 mm for the Envisat radar of wavelength 5.6 cm) between the spacecraft and the Earth's surface. The interferograms exhibit various topography sensitivity as measured by the altitude of ambiguity *ha* (Hanssen 2001)—the amount of unmodelled topography required to produce one fringe, and shown at the top right corner of each panel in Fig. 3 together with the time interval each differential interferogram spans. Figs 3(a)–(c) illustrate three independent short-term interferograms while Figs 3(d)–(f) cover longer time periods.

The dominant signal in the interferograms is a bowl-shaped pattern of apparent line-of-sight (LOS) displacements in the Mashhad area. All the short-term interferograms show roughly elliptical-shaped fringes directed northwest–southeast along the axis of the valley. The same fringe pattern can be traced in the interferometric pairs 3d–3f covering longer time intervals, though the fringe visibility there breaks down in the northern and northeastern part of the valley due to phase decorrelation. These decorrelation areas coincide with agricultural fields and vegetated parts of the valley, as observed on optical images and confirmed by field visits. Such areas render differential InSAR in the valley for time periods exceeding ~6 months.

The fringe pattern that we observe in Figs 3(a)–(f) can not be caused by unaccounted errors in topography as the number of fringes does not depend on the altitude of ambiguity (Bürgmann *et al.* 2000; Hanssen 2001). Because of the very steep incidence angle of the Envisat satellite and because of the evidence for vertical displacement in the valley from ground-truth observations, including levelling and GPS measurements, we interpret the elliptical-shaped fringes in Fig. 3 as indicating land subsidence in Mashhad Valley. The interferograms reveal that the spatial pattern of subsidence does not change over time. However, the amount of subsidence increases over longer time periods. For example, in the 140-d interferogram from 2004 June to November (Fig. 3c) we measure as much as 12 cm (four fringes) of land subsidence, whereas in the 385-d interferogram from 2004 November to 2005 November (Fig. 3d), spanning an ~2.5 times longer time interval, subsidence amounts to at least 27 cm (nine fringes). Due to the loss of coherent signal, it is difficult to assess exactly the maximum amount of subsidence in the long-term interferograms, but the data suggest that the rate of subsidence for this time interval is approximately constant. No significant seasonal variation is observed in the InSAR measurements during the 2003–2005 time interval.
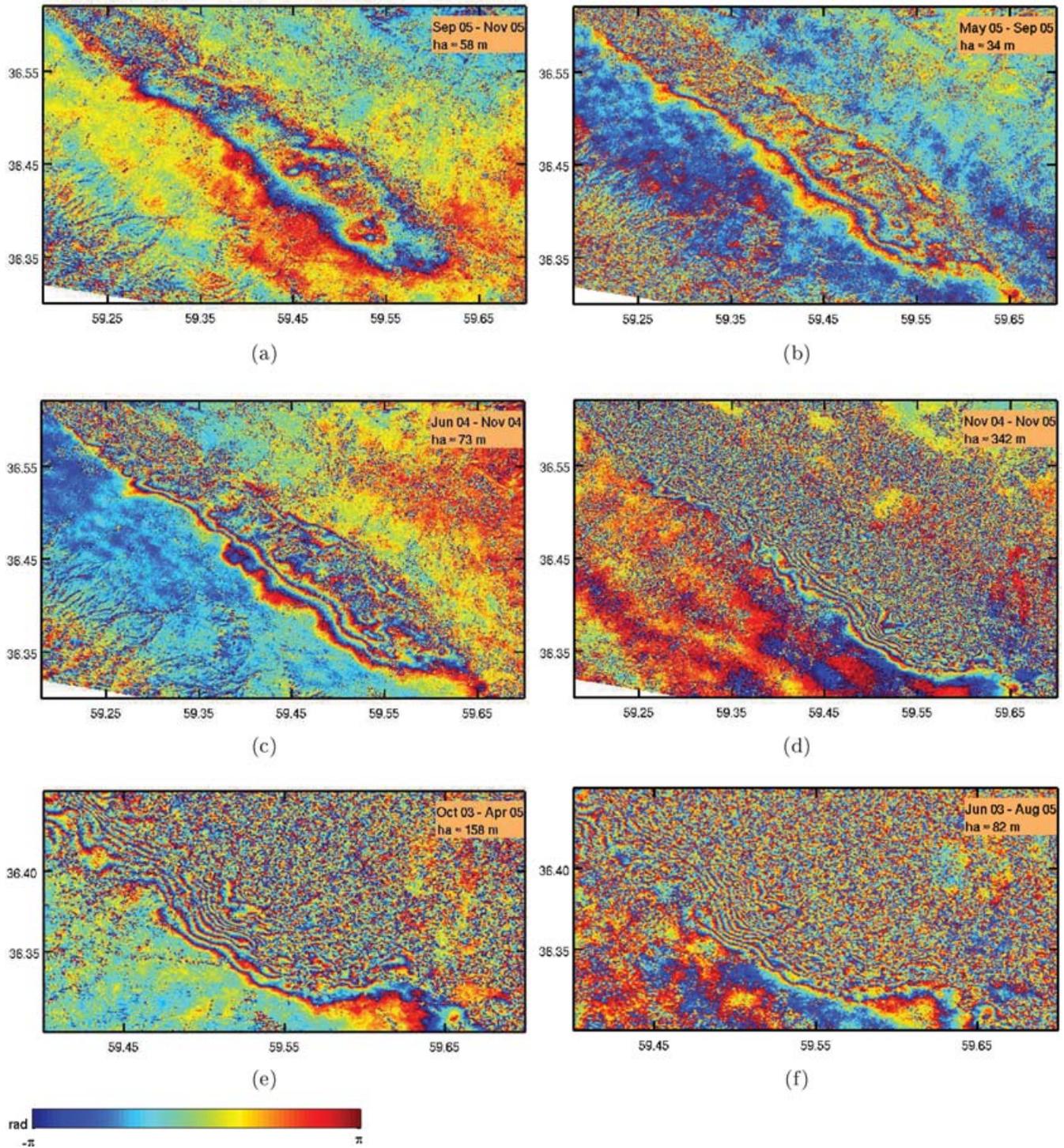
Figure 3. Six differential (wrapped) interferograms for the Mashhad area, showing spatial and temporal distribution of land subsidence in the region. The time interval appears in the upper right corner of each panel. h_a is the altitude of ambiguity in metres. One fringe represents 28 mm of range change. The dominant signal in the short-term interferograms (a)–(c) is an elliptical-shaped fringe pattern directed northwest–southeast along the axis of the valley. The fringe visibility in the long-term interferograms (d)–(f) breaks down in the northern and northeastern part of the valley due to phase decorrelation.

Assuming the rate of deformation is constant, at least over the time period being covered by our InSAR observations, and atmospheric errors are random, we generate a mean velocity map from 13 best interferograms with temporal separations between 70 and 770 d (Table 1). The phase of each interferogram is first unwrapped using a statistical minimum-cost flow algorithm implemented in the SNAPHU package (Chen & Zebker 2001), and calibrated such that the average displacements at the southern periphery of the inferred subsidence bowl are approximately zero. To obtain reliable unwrapped data we set a threshold of 0.2 on coherence values and restrict the unwrapping operation in the SNAPHU to involve only those pixels exhibiting an estimated coherence of higher than this
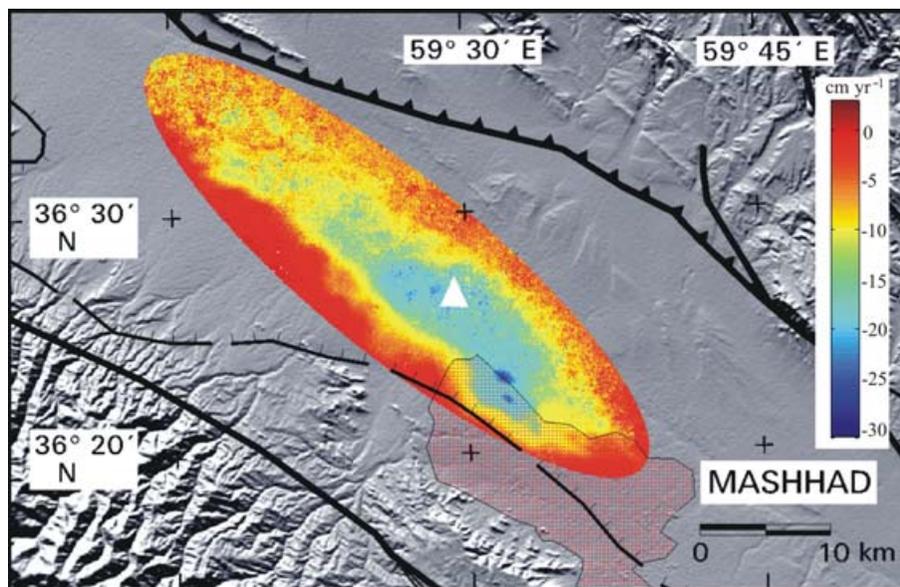
(a)
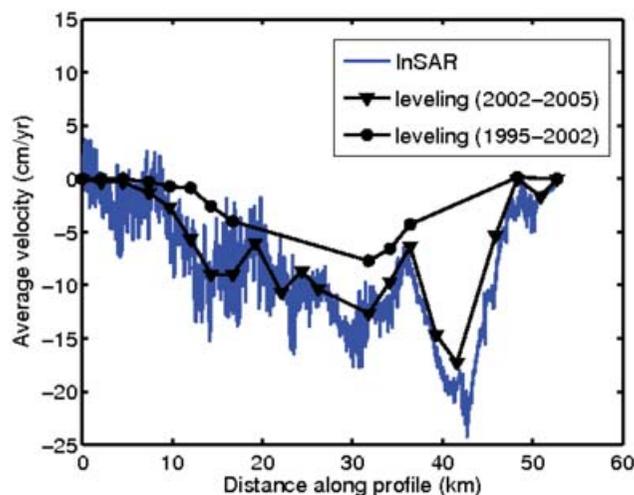
(b)

Figure 4. (a) A stack of 14 unwrapped interferograms listed in Table 1, overlying the geologic map, showing the mean velocity of land subsidence in the Mashhad region during two and a half years of InSAR observations. InSAR results outside the main subsiding area in the valley have been masked out for better illustration. The white triangle marks the location of the Tous GPS station. (b) Subsidence rates as measured by precise levelling and transect of the InSAR map in Fig. 4(a) along the levelling route shown in Fig. 1(a).

threshold. Image pixels with coherence values less than 0.2 are replaced by dummy values in the final unwrapped results. We then normalize the unwrapped interferograms by the time interval they span and stack them to obtain the mean velocity, the result of which is shown in Fig. 4(a).

Fig. 4(a) illustrates the mean subsidence rate for our study area in Mashhad during two and a half years of InSAR observations. The subsidence bowl generated from the stacking is cut and overlain on Fig. 1(a) to better signify its location and spatial extent with respect to surrounding geological features and the city of Mashhad. The InSAR map indicates that approximately 70 km^2 in the valley floor, including the northwestern part of Mashhad City, subsided at a rate exceeding 15 cm yr^{-1} between 2003 and 2005. As much as ∼28–30 cm yr^{-1} is inferred for the maximum rate of subsidence in this period. This makes the Mashhad valley as one of the most rapidly

subsiding areas in the world, approaching or even exceeding dimensions and rates observed at well-known groundwater basins and oilfields such as Las Vegas (Bell *et al.* 2002), New Orleans (Dixon *et al.* 2006) and the LOS Hills and Belridge oilfields (Fielding *et al.* 1998).

4 DISCUSSION

Comparison between the levelling results and InSAR data extracted from the stacked interferogram along the same transect shows that the vertical displacements inferred from the InSAR agrees well in both magnitude and trend with vertical displacements measured in the 2002–2005 levelling survey (Fig. 4b). InSAR results also show consistency with the average subsidence rate of 22 cm yr^{-1} at Tous GPS station (triangle in Fig. 4a), obtained from the 2005–2006

(a)

(b)
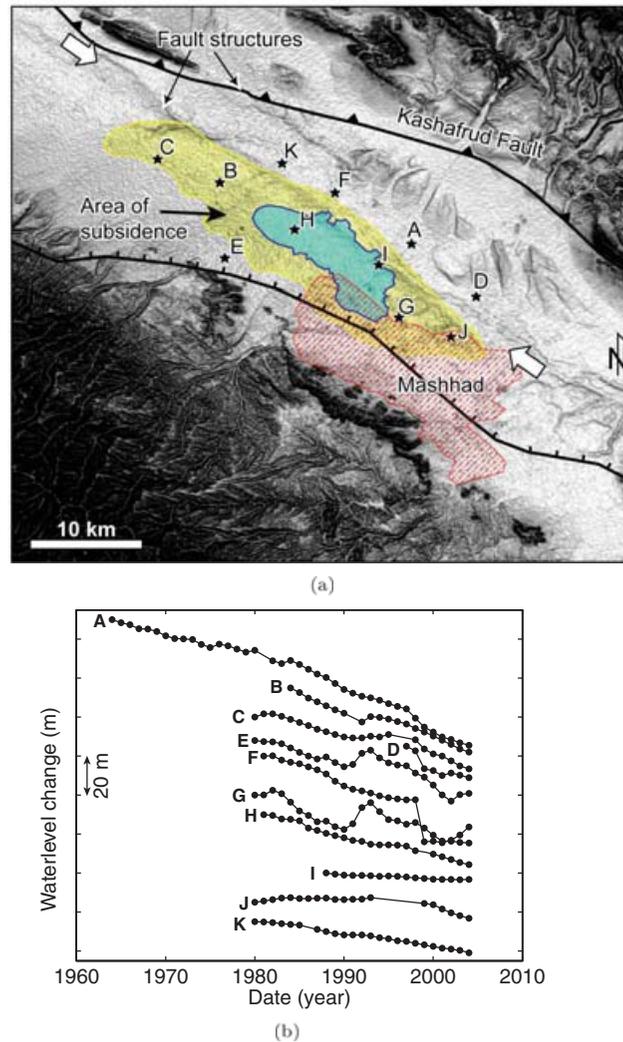
Figure 5. (a) Slope map of the Mashhad valley; steeper slopes are darker. Blue colour signifies the region with the rate of subsidence exceeding 15 cm yr^{-1} during 2003–2005. The yellow contour line delimits the spatial extent of $\sim$5 cm yr^{-1} of land subsidence in Mashhad Valley. White arrows indicate inferred Quaternary fault traces to the north of the subsidence zone. (b) Water-level change for 11 piezometric wells in Mashhad Valley. The locations of wells are marked by black asterisks in Fig. 5(a).

continuous GPS observations (Fig. 2b). However, a striking feature of Fig. 4(b) is the difference between the rate of subsidence inferred from the InSAR and the 2002–2005 observations, in comparison to that obtained by the 1996–2002 observations for levelling benchmarks along the profile. Because the time interval over which these observations were made are different we interpret such a difference in rate as an indication that the average rate of subsidence has increased in the subsiding area since 2002.

Aside from illustrating the spatial extent and magnitude of the rate of subsidence in the Mashhad area, Fig. 4(a) also shows the effect of a Quaternary NW–SE basin fault which passes through the city of Mashhad and creates a boundary for the subsidence. As one can see in Fig. 4(a), the subsidence bowl enters to the city from the northwest but stops as it approaches to this fault. Interestingly, morphological analysis of the Landsat Thematic Mapper and SRTM data reveals the presence of similar Quaternary fault traces at the northern margin of the subsidence zone outside Mashhad City (Fig. 5a). These detailed observations suggest that Quaternary structures (faults) that cut the valley floor might act in part as barrier to subsidence either by separating two different materials with, for

instance, differences in compressibility or by causing localization of water flows and deformation in homogenous materials even in the absence of compressibility contrasts (Bell *et al.* 2002). Simplified published geologic map of the Mashhad area does not show evidence for the contrast in surface lithology across basin faults in the valley floor. However, more detailed information about the stratigraphy of Quaternary sediments would be needed to exactly address such phenomenon and derive the effect of geological structures on the aquifer system at Mashhad.

To better understand the cause of land subsidence in Mashhad Valley we examine variations in groundwater levels at a few piezometric wells in the region. Groundwater level measurements have been made regularly in the valley since the beginning 1960s by the Water Management Organization of Mashhad. The number of piezometric wells throughout the whole valley has increased to 90 in 2004 from just 14 in 1964 (Anvari, personal communication, 2006). Analysis of groundwater tables at these wells indicates that subsidence most likely results from overdrafting of the underground aquifer system. Fig. 5(b) shows the behaviour of yearly mean piezometric records at 11 wells in and around the subsiding area. The locations

of wells have been marked by black asterisks in Fig. 5(a). From the time-series of piezometric records it is evident that a continuous lowering of the hydraulic head below the ground level has been occurring in the region over the past decades. The longest record of piezometric measurements is at well A; from 1964 to 2004, the water table at this well declined as much as 65 m as a resultant consequence of intensive groundwater pumping and deficient natural recharge.

Worldwide examples suggest a correlation between variation in water-table levels and land surface displacement, as well documented, for example, in Las Vegas Valley, Nevada (Hoffmann *et al.* 2001), Antelope Valley and Santa Clara Valley, California (Galloway *et al.* 1998; Schmidt & Bürgmann 2003), Jakarta City, Indonesia (Abidin *et al.* 2001) and the city of Paris, France (Mouelic *et al.* 2002). Subsidence bowls resulting from overdrafting of aquifer systems, however, do not always correlate spatially with regions of major pumping and maximum water-level decline (Galloway *et al.* 1999). In some cases (e.g. Las Vegas) maximum water level declines are offset from maximum subsidence, probably due to different compressibilities (Bell *et al.* 2002). There are also places such as Memphis, Tennessee, where no significant land subsidence was recorded despite the intensive decline in groundwater levels (Poland & Davis 1969). In principle, overabstraction of the groundwater creates pore-water pressure reduction within the aquifer-aquitard system which is reflected by an increase in the effective stress and compaction of sediments (Terzaghi 1925). The relationship between these two processes depends upon many factors, including geotechnical parameters such as sediment porosity, permeability and compressibility, the spatial distribution of thickness of compressible layers within the aquifer-aquitard system, and the history and amounts of pressure drawdown caused by groundwater decline (Freeze & Cherry 1979). Some external processes such as tide, recharge, or regional tectonics might also affect the aquifer system deformation (Amelung *et al.* 1999; Moreau *et al.* 2006)

In the Mashhad area, time-series of piezometric records clearly exhibit drastic drop of groundwater levels in the valley within the past decades. However, not all the piezometric wells for which a steady increase in the depth to water table has been recorded are located inside the subsidence bowl. For example, despite the water-level declines at wells A, D, E, F and K little if any significant subsidence is measured at these locations. Correlation between land subsidence and change in groundwater level appears to be better defined in general around wells B, C, G, H, J and I where we observe both land subsidence and a water level drawdown of several metres to tens of metres during the past years. Such a difference in the degree of correlation between subsidence and water-level change at various piezometric wells in the valley might be caused by spatial variation in the thickness and depth of fine-grained compressible layers (silt and clay) in the aquifer system, by the influence of geologic features such as faults on basin stratigraphy, or by other geotechnical parameters controlling the mechanics of deforming aquifer. Hydrostratigraphic mapping of subsurface sediments together with temporally and spatially dense observations of surface motions using techniques like InSAR, GPS and levelling would be vital to gain a better understanding of the causative links between variation in geotechnical and hydrological parameters and change in surface deformation at Mashhad. This matter requires further investigation for the years to come.

Unless improved groundwater management plans are implemented, it is anticipated that continued pressure on the groundwater resources in Mashhad Valley, as evidenced in the time-series of piezometric records in Fig. 5(b) with rates of extraction far beyond those of natural recharge, might cause serious damage to urban, agricultural and industrial areas in the region. Careful consideration and sustainable water resources management need to be developed to provide a framework to meet water demands of more than 2 million local inhabitants and over 12 million annual tourists and pilgrims, numbers which are significantly increasing in recent years. The maximum annual subsidence rate of 28–30 cm yr^{-1} inferred based on InSAR observations in this study is one of highest rate of deformation ever recorded for groundwater basins subject to groundwater development. Land subsidence and earth fissures resulting from overexploitation of water are serious geologic hazards and their impacts will increase as more water is withdrawn from aquifers in the Mashhad region without adequate replenishment.

5 CONCLUSION

We have used interferometric analysis of space-borne Envisat SAR to map land subsidence in Mashhad Valley, northeast Iran. InSAR observations reveal for the first time that the total area of subsidence appears as a roughly NW-SE elliptical-shaped bowl along the axis of the valley with a maximum annual rate of 28–30 cm yr^{-1} for the 2003–2005 time period. We have presented evidence from piezometric records surrounding the subsidence area indicating that such deformation likely results from overdrafting of the groundwater system. Water level decline of as much as 65 m was recorded in the region during the last four decades. The radar observations of land subsidence are in good agreement with recent levelling and GPS observations. However, the radar data provides a more detailed mapping of both the amplitude and spatial extent of land subsidence. In particular, the InSAR mapping reveals that the subsidence area infiltrates from the northwest to Mashhad City and that Quaternary faults control the spatial extent of the observed subsidence bowl along its southern and northern margin.

ACKNOWLEDGMENTS

REFERENCES

Abidin, H.Z. *et al.*, 2001. Land subsidence of Jakarta (Indonesia) and its geodetic monitoring system, *Nat. Hazards,* **23,** 365–387.

Altamimi, Z., Sillard, P. & Boucher, C., 2002. ITRF2000: A new release of the International Terrestrial Reference Frame for earth science applications, *J. Geophys. Res.,* **107**(B10), 2214, doi:10.1029/2001JB000561.

Amelung, F., Galloway, D. L., Bell, J. W., Zebker, H. A. & Laczniak, R. J., 1999. Sensing the ups and downs of Las Vegas–InSAR reveals structural control of land subsidence and aquifer-system deformation: *Geology,* **27,** 483–486.

Bell, J. W., Amelung, F., Ramelli, A. R. & Blewitt, G., 2002. Subsidence in Las Vegas, Nevada, 1935–2000: New Geodetic Data Show Evolution, Revised Spatial Patterns, and Reduced Rates, 2002. *Environ. Eng. Geosci.,* **8,** 155–174.

Bull, W.B. & Poland, J.F., 1975. Land subsidence due to ground-water withdrawal in the Los Banos-Kettleman City area, California; Part 3, Interrelations of water-level change, change in aquifer-system thickness, and subsidence: *US Geological Survey Professional Paper 437-G,* 62 p.

Bürgmann, R., Rosen, P. & Fielding, E., 2000. Synthetic aperture radar interferometry to measure Earth's surface topography and its deformation, *Annu. Rev. Earth planet. Sci., 28,* 169–209.

Bürgmann, R., Ayhan, M.E., Fielding, E.J., Wright, T.J., McClusky, S., Aktug, B., Demir, C., Lenk, O. & Türkezer, A., 2002. Deformation during the 12 November 1999 Düzce, Turkey, Earthquake from GPS and InSAR Data, *Bull. seism. Soc. Am., 92,* 161–171.

Chen, C.W. & Zebker, H.A., 2001. Two-dimensional phase unwrapping with use of statistical models for cost functions in nonlinear optimization, *J. Opt. Soc. Am. (Optics, Image Science and Vision) 18,* 338–351.

Dixon, T.H., Amelung, F., Ferretti, A., Novali, F., Rocca, F., Dokka, R., Sella, G., Sang-Wan Kim, Wdowinski, S. & Whitman, D., Subsidence and flooding in New Orleans, *Nature, 441,* 587–588.

Fialko, Y., 2006. Interseismic strain accumulation and the earthquake potential on the southern San Andreas fault system, *Nature, 441,* 968–971.

Fielding, E.J., Blom, R.G. & Goldstein, R.M., 1998. Rapid subsidence over oil fields measured by SAR interferometry. *Geophys. Res. Lett., 27,* 3215–3218.

Feigl, K.L. *et al.,* 1993. Space geodetic measurement of crustal deformation in central and southern California, 1984–1992, *J. geophys. Res., 98,* 21 677–21 712.

Freeze, R.A. & Cherry, J.A., 1979. *Groundwater,* Englewood Cliffs, N.J., Prentice-Hall, c1979. UCD Phys Sci GB1003.2.F73.

Galloway, D.L., Hudnut, K.W., Ingebritsen, S.E., Phillips, S.P., Peltzer, G., Rogez, F. & Rosen, P.A., 1998. Detection of aquifer system compaction and land subsidence using interferometric synthetic aperture radar, Antelope valley, Mojave Desert, California, *Water Resour. Res., 34,* 2573–2585.

Galloway, D.L., Jones, D.R. & Ingebritsen, S.E., 1999. Land subsidence in the United States: US Geological Survey Circular 1182, 175 p.

Goldstein, R.M. & Werner, C.L., 1998. Radar interferogram filtering for geophysical application, *Geophys. Res. Lett., 25,* 4035–4038.

Hanssen, R., 2001. *Radar Interferometry: Data Interpretation and Error Analysis,* Kluwer Academic Publishers, Netherlands.

Herring, T.A., 1998. *GLOBK: Global Kalman Filter VLBI and GPS Analysis Program,* Vol. 4.1, Mass. Inst. of Technol., Cambridge.

Hoffmann, J., Zebker, H.A., Galloway, D.L. & Amelung, F., 2001. Seasonal subsidence and rebound in Las Vegas Valley, Nevada, observed by synthetic aperture radar interferometry, *Water Resour. Res., 37,* 1551–1566.

Ikehara, M.E. & Phillips, S.P., 1994. Determination of land subsidence related to ground-water-level declines using global positioning system and leveling surveys in Antelope Valley, Los Angeles and Kern Counties, California: *US Geological Survey Water-Resources Investigations Report,* 101 p.

Kampes, B. & Usai, S., 1999. Doris: The Delft Object-oriented Radar Interferometric software. 2nd International Symposium on operationalization of Remote Sensing, ITC, Enschede, the Netherlands. 4 pages (on CD-ROM).

King, R.W. and Bock, Y., 1995. *Documentation of the GAMIT GPS Analysis Software,* Mass. Inst. of Technol., Cambridge.

Lanari, R., Lundgren, P., Manzo, M. & Casu, F., 2004. Satellite radar interferometry time series analysis of surface deformation for Los Angeles, California, *Geophys. Res. Lett., 31,* L23613, doi:10.1029/2004GL021294.

Longfield, T.E., 1932. The Subsidence of London:Ordnance Survey, Prof. Papers, new ser., no. 14.

Massonnet, D., Rossi, M., Carmona, C., Adragna, F., Peltzer, G., Feigl, K. & Rabaute, T., 1993. The displacement field of the Landers earthquake mapped by radar interferometry, *Nature, 364,* 138–142.

McClusky, S. & 27 coauthors., 2000. Global Positioning System constraints on plate kinematics and dynamics in the eastern Mediterranean and Caucasus, *J. Geophys. Res., 105*(B3), 5695–5720.

Memarzadeh, Y., 1998. Refraction effect and statistical analysis of the Iran first order precise leveling data, *Master thesis,* K.N. Toosi University of Technology, Iran.

Moreau, F., Dauteuil, O., Bour, O. & Gavrilenko, P., 2006. GPS measurements of ground deformation induced by water level variations into a granitic aquifer (French Brittany), *Terra Nova, 18,* 50–54.

Motagh, M., Klotz, J., Tavakoli, F., Djamour, Y., Arabi, S., Wetzel, H.-U., Zschau, J., 2006. Combination of precise leveling and InSAR data to constrain source parameters of the Mw = 6.5, 26 December 2003 Bam earthquake, *Pure Appl. Geophys., 163,* 1–18.

Mouelic S.L., Raucoules, D., Carnec, C., King, C. & Adragna, F., 2002., A ground uplift in the city of Paris (France) revealed by satellite radar interferometry, *Geophys. Res. Lett., 29,* 17, 1853, doi:10.1029/2002GL015630.

Peltzer, G., Rosen, P., Rogez, F. & Hudnut, K., 1998. Poro-elastic rebound along the Landers 1992 earthquake surface rupture, *J. geophys. Res., 103,* 30 131–30 145.

Poland, J.F., 1956. Land-surface Subsidence: US Geological Survey Open-File Report, 13 p.

Poland, J.F., ed., 1984. Guidebook to Studies of Land Subsidence due to Ground-Water Withdrawal: v. 40 of UNESCO Studies and Reports in Hydrology: Paris, France, United Nations Educational, Scientific and Cultural Organization, 305 p.

Poland, J.F. & Davis, G.H., 1969. Land subsidence due to withdrawal of fluids, *Rev. Eng. Geol., 2,* 187–269.

Scharroo, R. & Visser, P.N.A.M., 1998. Precise orbit determination and gravity field improvement for the ERS satellites, *J. geophys. Res., 103,* 8113–8127.

Simons, M., Fialko, Y. & Rivera, L., 2002. Coseismic deformation from the 1999 Mw 7.1 Hector Mine, California, Earthquake as inferred from InSAR and GPS observations, *Bull. seism. Soc. Am., 92,* 1390–1402.

Schmidt, D.A. & Bürgmann, R., 2003. Time dependent land uplift and subsidence in the Santa Clara valley, California, from a large InSAR data set, *J. geophys. Res., 108,* doi:10.1029/2002JB002267.

Terzaghi, K., 1925. Principles of soil mechanics, IV, settlement and consolidation of clay, *Eng. News Rec., 95*(3), 874–878.

Tolman, C.F. & Poland, J.F., 1940. Ground-water, salt-water infiltration, and ground-surface recession in Santa Clara Valley, Santa Clara County, California, *Am. Geophys. Union Trans.,* 23–34.

Zebker, H.A., Rosen, P.A., Goldstein, R.M., Gabriel, A. & Werner, C.L., 1994. On the derivation of coseismic displacement fields using differential radar interferometry: the Landers earthquake, *J. geophys. Res., 99,* 19 617–19 634.